19th International Conference on the Computation of Electromagnetic Fields

Technical Program

Compumag 2013

30 June–4 July 2013, Budapest, Hungary

PC6-4
Estimation of Acoustic Noise and Vibration in an Induction Machine considering Rotor Eccentricity
Do-Jin Kim, Hae-Joong Kim, Jung-Pyo Hong, Chul-Jun Park, Jin-Tai Chung
Hanyang University, Republic of Korea (South Korea)

PC6-5
Nonlinear Dynamic Characteristic Analysis of Linear Actuator for Compressor
Sung-An Kim, Sang-Geon Lee, Yun-Hyun Cho
Dong-A University, Republic of Korea (South Korea)

PC6-6
Design of Hybrid Hysteresis Motor Rotor by Means of FE Model and Decision Process
Mariusz Jagiela, Tomasz Garbiec, Marcin Kowol
Opole University of Technology, Poland

PC6-7
Brushless Doubly-Fed Reluctance Machine Optimization using Reluctance Networks
Tiago Staudt[1,2], Lisa Scanu[1,2], Frédéric Wurtz[2], Nelson Jhoe Batistela[1], Patrick Kuo-Peng[1], Nelson Sadowski[1]
[1]Federal University of Santa Catarina (GRUCAD-UFSC), Brazil; [2]Grenoble INP-UJF, CNRS UMR 5529 (G2ELAB), France

PC6-8
Internally Consistent Nonlinear Behavioural Model of a PM Synchronous Machine for Hardware-in-the-Loop simulation
Derek N. Dyck[1], Tanvir Rahman[1], Christian Dufour[2]
[1]Infolytica Corp., Montreal; [2]2Opal-RT Technologies Inc., Montreal, Canada

PC6-9
Electromagnetic Performance Analysis of Axial Field Flux-Switching Permanent Magnet Machine Using Equivalent Magnetic Circuit Method
Da Xu[1,2], Mingyao Lin[1,2], Xinghe Fu[1,2], Li Hao[1,2], Xuming Zhao[3]
[1]School of Electrical Engineering, Southeast University, Nanjing, People's Republic of China; [2]Engineering Research Center for Motion Control of MOE, Southeast University, Nanjing, People's Republic of China; [3]Jiangsu Electric Power Maintenance Branch Company, Nanjing, People's Republic of China

PC6-10
Permanent Magnet Eddy Current Comparison of Surface Permanent Magnet Synchronous Motors with Different Permanent Magnet Shapes
Sun Kwon Lee[1,2], Gyu Hong Kang[1], Jin Hur[2], Byoung Woo Kim[2]
[1]Korea Marine Equipment Research Institute, Republic of Korea (South Korea); [2]University of Ulsan, Republic of Korea (South Korea)

PC6-11
Torque-Slip Characteristic of Squirrel Cage Induction Motor by New FEA Technique
Olivian Chiver, Liviu Neamt, Cristian Barz, Dumitru Pop
Technical Univerity of Cluj Napoca, Romania

Estimation of Acoustic Noise and Vibration in an Induction Machine Considering Rotor Eccentricity

Do-Jin Kim[1], Hae-Joong Kim[1], Jung-Pyo Hong[1], Chul-Jun Park[2]

[1]Department of Automotive Engineering, Hanyang University, Seoul 133-791, Republic of Korea
[2]Department of Mechanical Engineering, Hanyang University, Ansan 426-791, Republic of Korea

In this paper, a static rotor eccentricity analysis method is proposed. Electromagnetic noise by static eccentricity occurs in the course of manufacturing. The increase in errors is attributed to manufacturing errors of the components: the assembly error and the torsional error caused by shrink-fitting. For these reasons, the rotor is displaced from the center of the stator bore, but it still turns on its own axis. Accordingly, in this study, the acoustic noise using the electromagnetic excitation force was analyzed according to the rotor eccentricity. Finite element analysis (FEA) was used to analyze the rotor eccentricity considering the electrical and mechanical characteristics. To verify the proposed method, an induction machine was fabricated and an experiment was conducted.

***Index Terms*—Acoustic noise, electromagnetic excitation force, induction machine, rotor eccentricity, spectral analysis**

I. Introduction

ELECTRIC motors are among the most fundamental motion generation mechanisms in both industrial and household products. Although there are various types of electric motors, induction machines are the most popular due to their low cost and ease of operation. Much effort has been exerted of late to find the most suitable motor for a certain application and existent drive system. In addition, both environmental issues and the demand for low-noise induction machines have increased. In this regard, various researches on the reduction of noise and vibration of induction machines have been conducted for many years. The vibrations are measured on the surface of the motor frame together with the sound pressure levels around the motor, and then the measurements are analyzed in connection with the modal properties of the motor structure and electromagnetic excitation mechanisms [l-3].

In the analytical studies, the estimation of the Maxwell stress acting on the stator due to the magnetic flux in the air gap is the major concern. The Maxwell stress can be estimated using the classical electromagnetic excitation force and permeance wave theory [4-6], but the effects of the vibration and noise are not predicted. Accordingly, finite element analysis (FEA) was used in this study due to the effects considering the saturation factor and current waveform.

Rotor eccentricity is a fault that mainly affects induction machines. In the worst-case scenario, an eccentricity fault can result in a stator rotor rub, thereby causing severe damage to the motor as well as acoustic noise and vibration. The creation of an unequal air gap may involve many different factors, including (a) unbalanced load, (b) bearing wear, (c) bent rotor shaft, (d) mechanical resonance at the critical load, and (e) manufacture and assembly tolerance.

In this study, the noise of the induction machine with rotor eccentricity was calculated using the electromagnetic excitation force and mechanical analysis. First, the force was calculated via two-dimensional (2D) FEA analysis considering the saturation factor, the current waveform, and the changing rotor eccentricity. Second, the natural frequency of the induction machine was calculated for the mechanical characteristics. Third, the electromagnetic excitation force, mechanical characteristics such as the natural frequency of each mode, and deformation of the stator and noise were calculated via FEA. The calculated spectrum using the air gap flux density was analyzed to determine the effects of eccentricity.

The motor consisted of two poles, 24 stator slots, and 31 rotor slots at 3.7 kW rated power. To change the quantity of the static rotor eccentricity, the motor was fabricated using a bolt on the front and back housing. The acoustic noise and the vibration of the motor were measured in a motor-based test at the no-load condition to eliminate the noise generated by the dynamo.

TABLE I
SPECIFICATIONS OF THE TESTED MOTOR

List	Values
Phase/pole	3/2
Rated output power	3.7 kW
Voltage/frequency	220V/60 Hz
Number of slots (stator/rotor)	24/31
Winding method	Distribution winding (short pitch: 5/6)
No-load current	6.0 A
Skew	Rotor 3.1°

II. Analysis Method

The specifications of the induction machine are shown in Table I. The motor consisted of two poles, 24 stator slots, and 31 rotor slots at 3.7 kW rated power.

To reduce the harmonic components, the winding pitch was set at 9, as shown in Fig. 1, and a skewed rotor was employed to reduce the harmonic components. The acoustic noise of the induction machine was measured in a motor-based test at the no-load condition, according to the quantity of the static eccentricity. Therefore, 2D analysis was conducted under experimental conditions.

Manuscript received June 20, 2013. Corresponding author: Jung-Pyo Hong (e-mail: hongjp@hanyang.ac.kr
Digital Object Identifier inserted by IEEE

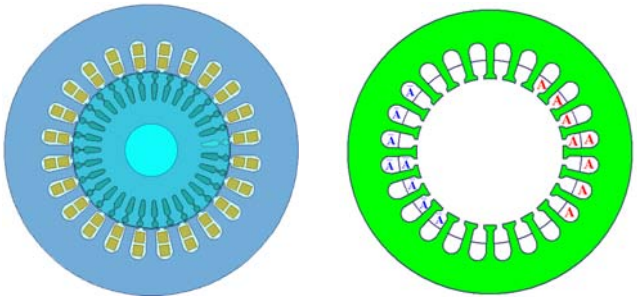

(a) (b)

Fig. 1. Configuration of the 3.7kW induction machine: (a) cross-section view; and (b) short-pitch winding of phase A (9/12).

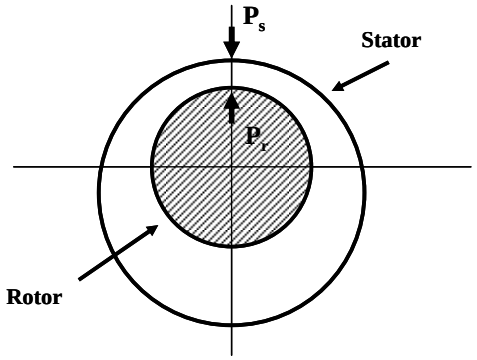

Fig. 2. Cross-section view of a motor with static eccentricity.

A. *Variable Time-stepping FEM*

To consider the flux density, which is affected by time, time-stepping FEM was used for the analysis of the magnetic field [7]. The governing equation for 2D FEA is given by

$$\frac{\partial}{\partial x}\left(\frac{1}{\mu}\frac{\partial A}{\partial x}\right)+\frac{\partial}{\partial y}\left(\frac{1}{\mu}\frac{\partial A}{\partial y}\right)=\sigma\frac{dA}{dt}-J_0, \tag{1}$$

where A is the z-component of the magnetic vector potential, μ is the permeability, σ is the conductivity of the materials, and J_0 is the exciting current density of the stator winding.

$$V_a = I_a R_a + L_e\frac{dI_a}{dt}+\frac{d\phi_a}{dt}, \tag{2}$$

where V_a, I_a, R_a, and ϕ_a are the voltage, current, resistance, and flux linkage, respectively. L_e is the end coil inductance calculated using the equivalent method.

B. *Skew effect*

In this model, a skewed rotor is employed in the induction machines. When a skewed rotor is employed, the current waveform for the skewed model, $i_s(t)$, corresponding to the total current, can be obtained using equation (3). The higher harmonic components of the skewed rotor are smaller than the no skewed model. The noise of the skewed model was reduced due to the reduction of the harmonic components that affect the noise [8].

$$i_s(t)=\sum_{k=1}^{N}\frac{\Delta L}{L}\{i(t+\Gamma)\}, \tag{3}$$

where

$$\Gamma=\frac{\Delta\theta\cdot 60}{N\cdot 360}p=\frac{(k-1)\Delta\theta}{6N}\cdot p\cdot \tag{4}$$

N is the rotor speed in rpm, $\Delta\theta$ is the slice angle, L is the stack length of the motor, ΔL is the stack length of the single slice, and p is the pole pair.

C. *Electromagnetic excitation force*

Spectrum analysis was performed for the air gap flux density, which consists of the time and space harmonics. The radial force calculated from the air gap flux density was analyzed using a Fourier series.

$$F(\alpha,t)=\sum_{\nu}\sum_{l}F_{\nu,l}\cos\left(\nu p\alpha\mp l\omega t+\alpha_{\nu,l}\right), \tag{5}$$

where $F_{\nu,l}$ is the magnitude of the k space harmonic component, l is the time harmonic component, ω is the fundamental angular frequency of the phase voltage, α is the circumferential position of the air gap, and $\alpha_{k,l}$ is the phase angle of the electromagnetic force. The stator deformation mode and frequency occurred due to the space and time harmonic components, respectively. In the case of the pure static eccentricity illustrated in Fig. 3, the position of the radial minimal air gap length was fixed in space. To consider the static eccentricity, the variation of the air gap around the magnetic circuit periphery and with the time is

$$g(\alpha,t)=g\left[1-\varepsilon\cos\left(\alpha-\omega_\varepsilon t\right)\right], \tag{6}$$

where $g=R-r$, R is the inner stator core radius, and r is the outer rotor radius. The equation is $\varepsilon=e/g$. e. The rotor eccentricity, g, is an ideal uniform air gap.

In the case of the no-eccentricity model, the 2nd and 31st time harmonic components were produced by pole number and stator-rotor slot combination. The time harmonics are

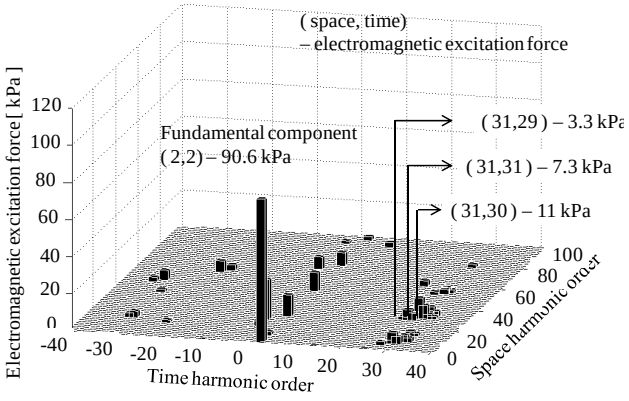

Fig. 3. Spectrum analysis of the no-eccentricity model.

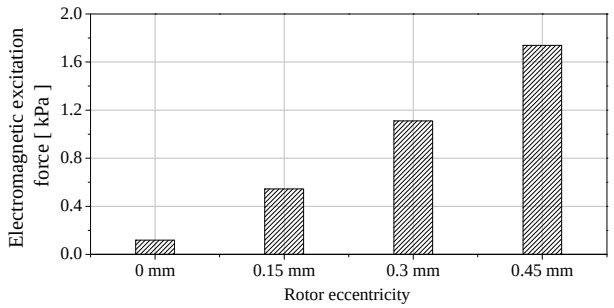

(a)

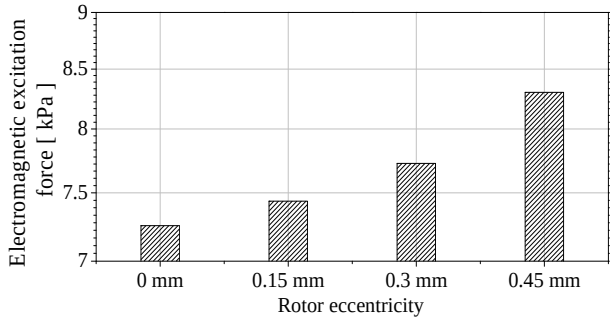

(b)

Fig. 4. Electromagnetic excitation force according the rotor eccentricity (a) 1st space, 2nd time harmonic component, and (b) 31st space, 31st time harmonic component.

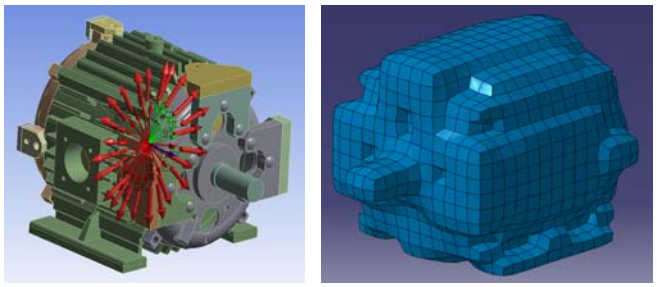

(a) (b)

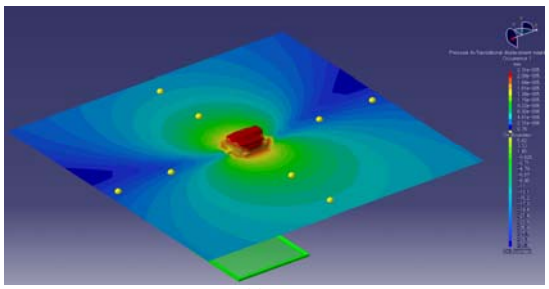

(c)

Fig. 5. FEA simulation for calculating the noise of the motor: (a) force injection; (b) motor modeling of the acoustic noise simulation; and (c) simulation result.

directly related to the frequency of the acoustic noise and vibration.

In the case where the rotor had static eccentricity, the 1st harmonic component was increased as the complex components that are produced by even harmonics produced from the eccentricity and the fundamental component. The 1st and 31st forces affected the noise and vibration. To understand the efforts of the static rotor eccentricity, the calculated simulation results of the time and space harmonic components are compared in Fig. 4.

D. Natural frequencies

To consider the mechanical characteristics and resonance, the natural frequency and mode of each component of the motor assembly were calculated via FEA, with the material and geometry. The components of the motor, such as the rotor assembly, stator assembly with housing, and motor assembly, and the designed model, can avoid motor resonance by mismatching the frequency of the electromagnetic excitation force to the mechanical natural frequency.

E. Noise simulation

The distribution of the radiated noise was identified using acoustic analysis. The noise in a high-frequency region was used to analyze the distribution of the radiation. The acoustic noise was simulated using an LMS Virtual Lab. Harmonic acoustic analysis was conducted using modal-based force response analysis from the electromagnetic excitation force. The components of the radial force were calculated on the air gap that was put in the tooth of the stator according to the rotor position. The measurement points of the noise in the simulation are similar to the actual case data at the no-load condition. The result of the noise simulation is shown in Fig. 5.

III. EXPERIMENT

To verify the proposed method, a motor was fabricated using a bolt on the front and back housing. The natural frequency of each component and motor assembly were measured, and the results obtained were compared with the FEA results in Table II. To measure the quantity of the static rotor eccentricity, a dial gauge was installed in the front and back parts of the motor.

To shed light on the eccentricity effect tendency, the quantity of the rotor eccentricity was determined considering the air gap. The quantity of the rotor eccentricity was measured using the dial gauge from the shaft, and is shown in Fig. 6. The experiment setup, which was set in a soundproof room to reduce the external efforts, is shown in Fig. 7. A motor test was conducted under the no-load condition to eliminate the noise generated by the dynamometer. A microphone was installed on one side and at the front part of the motor. To
verify the proposed process, the measured noise and the FEA analysis result were compared, as shown in Fig. 8 and 9. The

(a) (b)

Fig. 6. Experimental setup for measuring the eccentricity: (a) dial gauge at the front part of the motor; and (b) dial gauge at the back part of the motor.

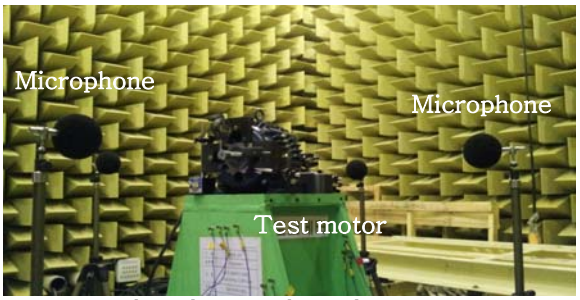

Fig. 7. 3.7kW induction machine undergoing a noise test.

noise that occurred due to the rotor, stator slots, and eccentricity combination was increased by the rotor eccentricity. Table III shows the results of the FEA and experiment.

IV. Conclusion

In this paper, a static rotor eccentricity analysis method is proposed, and its effects are analyzed by considering the electrical and mechanical characteristics. The influence of the rotor eccentricity on the magnetic forces acting on the stator surface on the harmonic spectrum of these forces and on the noise level of the machine is shown. Comparison from the simulation results obtained via FEA was made for the no-eccentricity case and for the case where the eccentricity level was changed for a 3.7kW induction machine. According to the efforts of the rotor eccentricity, the 1st and 31st harmonic time harmonic components increased. The 1st and 31st harmonic components of the acoustic noise occurred, and the rotor eccentricity was considered.

Acknowledgement

This research was supported by MSIP (Ministry of Science, ICT, & Future Planning), Republic of Korea, under the C-ITRC (Convergence Information Technology Research Center) support program (NIPA-2013-H0401-13-1008) supervised by NIPA (National IT Industry Promotion Agency).

V. Reference

[1] S C Chang, and R Yacamini, "Experimental study of the vibrational behaviour of machine stator", *IEE Proc., Electr. Power Appl.*, 143, (3), pp 242-250, 1996

[2] F., Kako, T., Tsuruta, K., Nagaishi, and H., Kohmo, "Experimental study on magnetic noise of large induction motors", *IEEE Trans* , PAS-102, (8), pp 2805-2810, 1983

[3] K. J. Kim, Y. S. Park, D. H. Cho and H. Lee, "Experimental analysis of noise and vibration of integral horse power induction motors", Internoise '95, Newport Beach, *CA*, pp 105-108, July 1995

[4] S. J. Yang, Low-noise electrical motors, Clarendon Press, Oxford, 1981

[5] P. L. Timar, A. Fazekas, J. Kiss, A. Miklos, S. J. Yang, Noise and vibration of electrical machines, Elsevier Science, 1989

[6] S. D. Garvey, M. I. Friswell and I. E. Penny, "The response of electrical machine stators to magnetic forcing", Thirteenth *IMAC*, Nashville, TN, pp. 1563-1569, 1995

[7] J. J. Lee, Y. K. Kim, H. Nam, K. H. Ha, J. P. Hong, and D. H. Hwang, "Loss Distribution of Three-Phase Induction Motor Fed by Pulse width-Modulated Inverters," *IEEE Trans. Magn.*, vol. 40, no. 2, pp. 762–766, Mar. 2004.

[8] D. J. Kim, J. W. Jung, J. P. Hong, K. W. Kim and C. J. Park, "A Study on the Design Process of Noise Reduction in Induction Motors," *IEEE Trans. Magn.*, vol. 48, no. 11, pp. 4638–4641, Nov. 2012.

TABLE II
Mechanical Natural Frequency Test Results

Frequency		Experiment [Hz]	FEA [Hz]
Rotor with shaft	1st mode	1140	1196
	2nd mode	2050	1981
Stator with winding	1st mode	1440	1508
	2nd mode	1880	1872
motor assembly	1st mode	1890	1698
	2nd mode	3160	3296

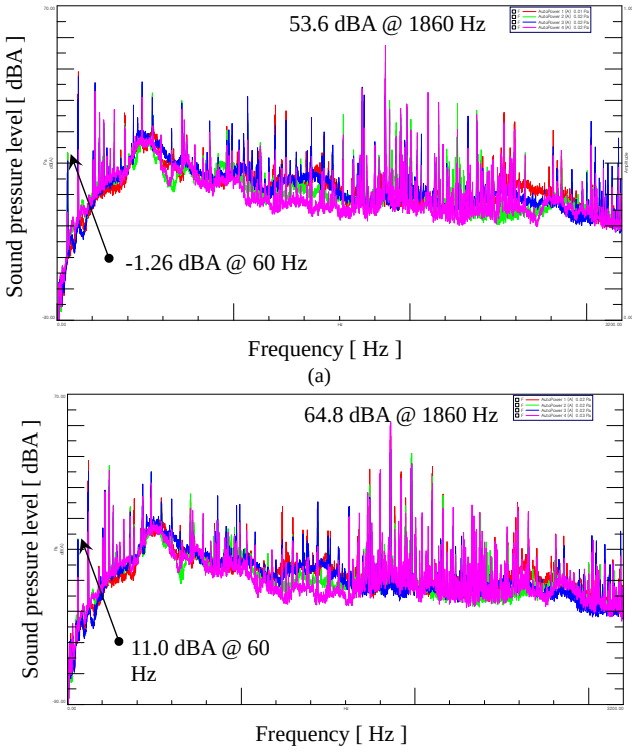

Fig. 8. Frequency spectrum of the measured noise: (a) noise spectrum analysis @ no eccentricity; and (b) noise spectrum analysis @ static eccentricity.

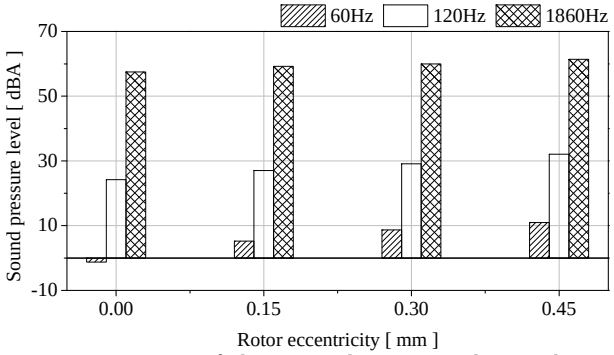

Fig. 9. Acoustic noise of the measured noise according to the rotor eccentricity and frequency.

TABLE III
Acoustic Noise of the Motor in the No-Load Condition

Eccentricity Value [mm]	Noise @ 1860 Hz [dB]	
	Experiment	FEA
0	53.6	-
0.15	59.5	60.0
0.30	61.7	61.1
0.45	64.8	65.4